

Thermal dileptons in high-energy nuclear collisions

Sanja Damjanovic
CERN, 1211 Geneva 23, Switzerland

November 1, 2018

Abstract

Clear signs of excess dileptons above the known sources were found at the SPS since long. However, a real clarification of these observations was only recently achieved by NA60, measuring dimuons with unprecedented precision in 158A GeV In-In collisions. The excess mass spectrum in the region $M < 1$ GeV is consistent with a dominant contribution from $\pi^+\pi^- \rightarrow \rho \rightarrow \mu^+\mu^-$ annihilation. The associated ρ spectral function shows a strong broadening, but essentially no shift in mass. In the region $M > 1$ GeV, the excess is found to be prompt, not due to enhanced charm production. The inverse slope parameter T_{eff} associated with the transverse momentum spectra rises with mass up to the ρ , followed by a sudden decline above. While the initial rise, coupled to a hierarchy in hadron freeze-out, points to radial flow of a hadronic decay source, the decline above signals a transition to a low-flow source, presumably of partonic origin. The mass spectra show the steep rise towards low masses characteristic for Planck-like radiation. The polarization of the excess referred to the Collins Soper frame is found to be isotropic. All observations are consistent with a global interpretation of the excess as thermal radiation. We conclude with a short discussion of a possible link to direct photons.

Introduction

Dileptons are particularly attractive to study the hot and dense QCD matter formed in high-energy nuclear collisions. In contrast to hadrons, they directly probe the entire space-time evolution of the expanding system, escaping freely without final-state interactions. At low masses $M < 1$ GeV (LMR), thermal dilepton production is mediated by the broad vector meson ρ (770) in the hadronic phase. Due to its strong coupling to the $\pi\pi$ channel and the short life time of only 1.3 fm/c, “in-medium” modifications of its mass and width close to the QCD phase boundary have since long been considered as the prime signature for *chiral symmetry restoration* [1, 2, 3]. At intermediate masses $M > 1$ GeV (IMR), it has been controversial up to today whether thermal dileptons are dominantly produced in the earlier partonic or in the hadronic phase, based here on hadronic processes other than $\pi\pi$ annihilation. Originally, thermal emission from the early phase was considered as a prime probe of *deconfinement* [4, 5].

Excess dileptons above the known decay sources at SPS energies were observed before by CERES [6, 7] for $M < 1$ GeV, NA38/NA50 [8] for $M > 1$ GeV and by HELIOS-3 [9] for both mass regions (see [10] for a short recent review including the preceding pp era and the theoretical milestones). The sole existence of an excess gave a strong boost to theory, with hundreds of publications. In the LMR region, $\pi\pi$ annihilation with regeneration and strong in-medium modifications of the intermediate ρ during the fireball expansion emerged as the dominant source. However, the data quality in terms of statistics and mass resolution remained largely insufficient for a precise assessment for the in-medium spectral properties of the ρ . In the IMR region, thermal sources or enhanced charm production could

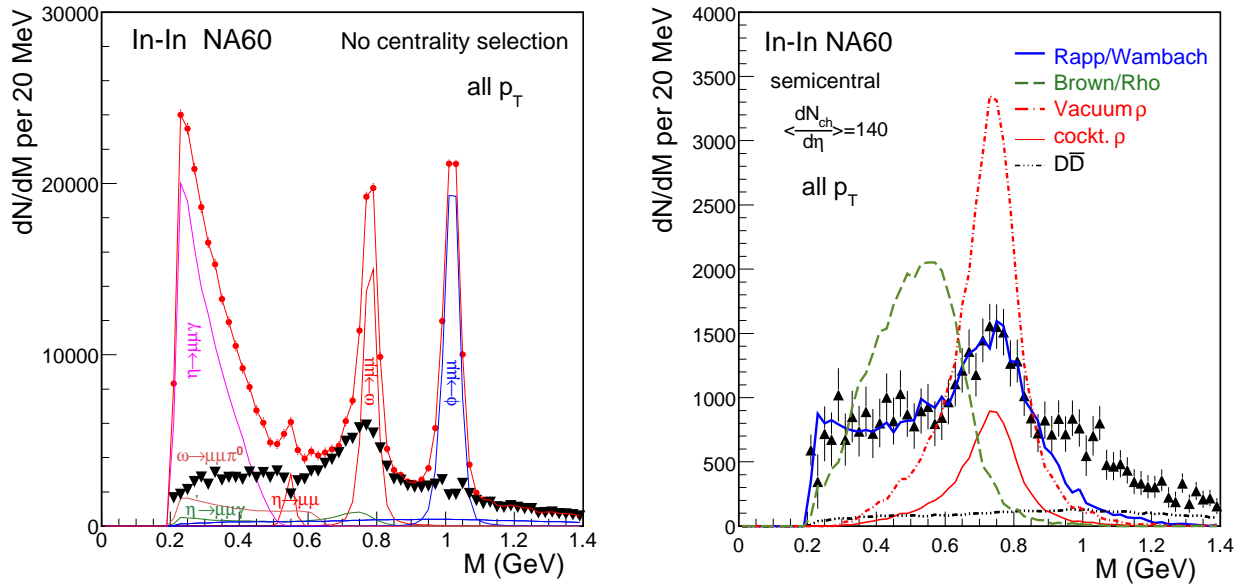


Figure 1: Left: Background-subtracted mass spectrum before (dots) and after subtraction of the known decay sources (triangles). Right: Excess dimuons compared to theoretical predictions [17], renormalized to the data in the mass interval $M < 0.9$ GeV. No acceptance correction applied.

account for the excess equally well, but that ambiguity could not be resolved, nor could the nature of the thermal sources be clarified.

A big step forward in technology, leading to completely new standards of the data quality in this field, has recently been achieved by NA60, a third-generation experiment built specifically to follow up the open issues addressed above [11]. Results on mass and transverse momentum spectra of excess dimuons have already been published [11, 12, 13]. Further aspects associated with the centrality dependence, polarization and acceptance-corrected mass spectra were reported during 2008 [14, 15]. This paper shortly reviews the central results and also discusses a possible link of the excess dileptons at very low masses to real photons.

Mass and p_T spectra of excess dileptons

Fig. 1 (left) shows the centrality-integrated net dimuon mass spectrum for 158A GeV In-In collisions in the LMR region. The narrow vector mesons ω and ϕ are completely resolved; the mass resolution at the ω is 20 MeV. The peripheral data can fully be described by the electromagnetic decays of neutral mesons [12, 16]. This is not true for the more central data as plotted in Fig. 1, due to the existence of a strong excess of pairs. The high data quality of NA60 allows to isolate this excess with *a priori unknown characteristics* without any fits: the cocktail of the decay sources is subtracted from the total data using *local* criteria, which are solely based on the mass distribution itself. The ρ is not subtracted. The excess resulting from this difference formation is illustrated in the same figure (see [12, 13, 16] for details and error discussion).

The common features of the excess mass spectra can be recognized in Fig. 1 (right). A peaked structure is always seen, residing on a broad continuum with a yield strongly increasing with centrality (see below), but remaining essentially centered around the nominal ρ pole [16]. Without any acceptance correction and p_T selection, the data can directly be interpreted as the *space-time averaged spectral function* of the ρ , due to a fortuitous cancellation of the mass and p_T dependence of the acceptance filtering and the phase space factors associated with thermal dilepton emission [16]. The two main theoretical scenarios for the in-medium spectral properties of the ρ , broadening [2] and dropping mass [3],

are shown for comparison [17]. Clearly, the broadening scenario gets close, while the dropping mass scenario in the version which described the CERES data reasonably well [2, 3, 6] fails for the much more precise NA60 data.

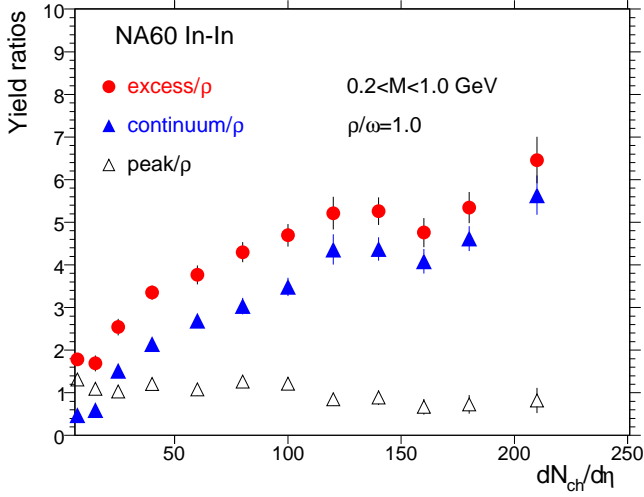


Figure 2: Excess yield ratios for peak, continuum and total vs. centrality for the mass window $0.2 < M < 1.0$ GeV and all p_T .

A detailed view of the shape of the excess mass spectra is obtained by using a side window method [16] to determine separately the yields of the peak and the underlying continuum. Fig. 2 shows the centrality dependence of these variables: peak, underlying continuum and total yield in the mass interval $0.2 < M < 1.0$ GeV, all normalized to the cocktail ρ . The continuum and the total show a very strong increase, starting already in the peripheral region, while the peak slowly decreases from >1 to <1 . Recalling that Fig. 1 roughly represents the full ρ spectral function, the excess/ ρ ratio can directly be interpreted as the number of ρ generations created by formation and decay during the fireball evolution, including freeze-out: the ' ρ -clock', frequently discussed in the past. It reaches up to about 6 generations for central In-In collisions; selecting lower p_T this number doubles.

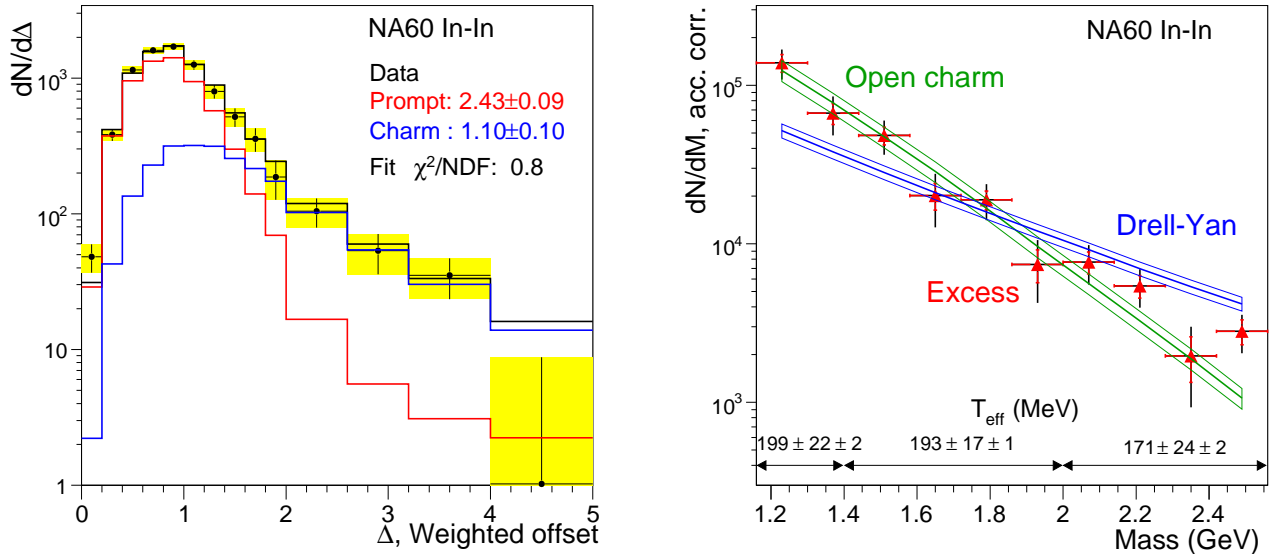


Figure 3: Left: Fit of the weighted offset distribution in the IMR region with the contributions from charm and prompt decays. Right: Acceptance-corrected mass spectra of Drell-Yan, open charm and the excess (triangles).

The central NA60 results in the IMR region [11] are shown in Fig. 3. The use of the *Si*-vertex tracker allows to measure the offset between the muon tracks and the main interaction vertex and

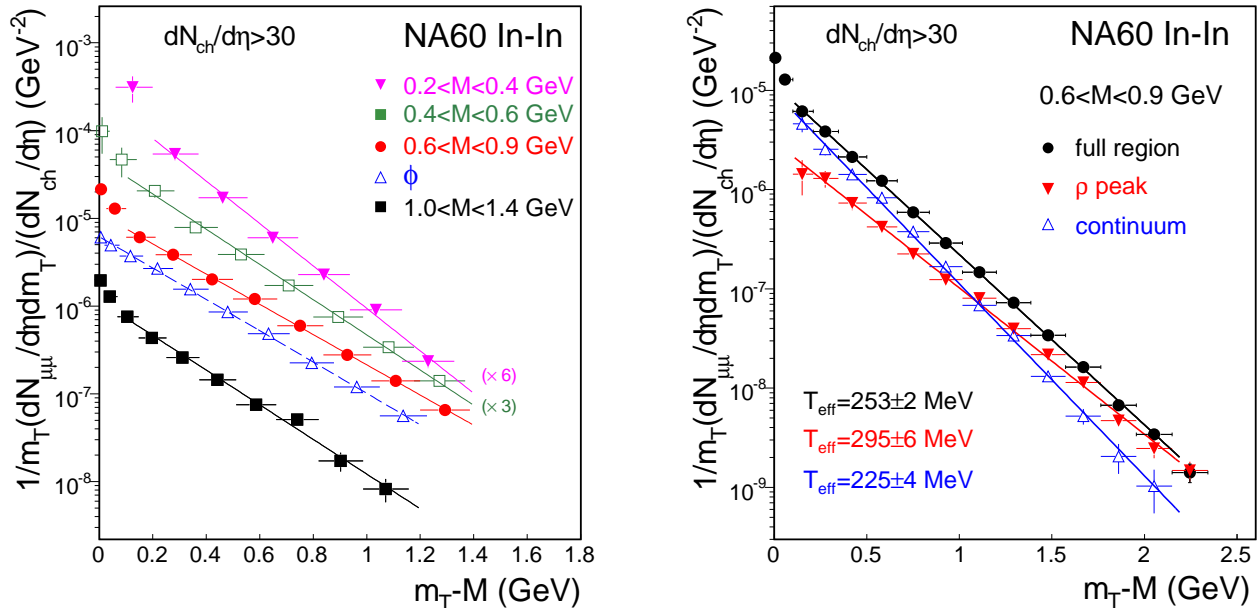


Figure 4: Acceptance-corrected transverse mass spectra of the excess dimuons for 4 mass windows and the ϕ [13] (left), and a decomposition into peak and continuum for the ρ -like window (right, see text). The lines represent exponential fits to the data in the range $0.4 < p_T < 1.8 \text{ GeV}$. The normalization in absolute terms is independent of rapidity over the region measured. For error discussion see [13].

thereby to disentangle prompt and offset dimuons from D decays. The left panel of Fig. 3 shows the offset distribution to be perfectly consistent with no charm enhancement, expressed by a fraction of 1.1 ± 0.1 of the canonical level. The observed excess is really prompt, with an enhancement over Drell-Yan by a factor of 2.4. The excess can now be isolated in the same way as was done in the LMR region, subtracting the measured known sources, here DY and open charm, from the total data. The right panel of Fig. 3 shows the decomposition of the total into DY, open charm and the prompt excess. The mass spectrum of the excess is quite similar to the shape of open charm and much steeper than DY; this explains of course why NA50 could describe the excess as enhanced open charm. The transverse momentum spectra are also much steeper than DY [11]. The fit temperatures of the m_T spectra associated with 3 mass windows are indicated on the bottom of the figure.

The remainder of this paper is solely concerned with excess data fully corrected for acceptance and pair efficiencies [13, 18]. In principle, the correction requires a 4-dimensional grid in the space of M - p_T - y - $\cos\theta_{CS}$ (where θ_{CS} is the polar angle of the muons in the Collins Soper frame). To avoid large statistical errors in low-acceptance bins, it is performed instead in 2-dimensional M - p_T space, using the measured y and $\cos\theta$ distributions as an input. The latter are, in turn, obtained with acceptance corrections determined in an iterative way from MC simulations matched to the data in M and p_T . The y -distribution is found to have the same rapidity width as $dN_{ch}/d\eta$, $\sigma_y \sim 1.5$ [18]. The $\cos\theta_{CS}$ distributions for two mass windows of the excess and the ω are contained in [14]. Within errors, they are found to be uniform, implying the polarization of the excess dimuons to be zero, in contrast to DY and consistent with the expectations for thermal radiation from a randomized system.

The two major variables characterizing dileptons are M and p_T , and the existence of two rather than one variable as in case of real photons leads to much richer information. Beyond (minor) contributions from the spectral function, p_T encodes the key properties of the expanding fireball, temperature and transverse (radial) flow. In contrast to hadrons, however, which receive the full asymptotic flow at the

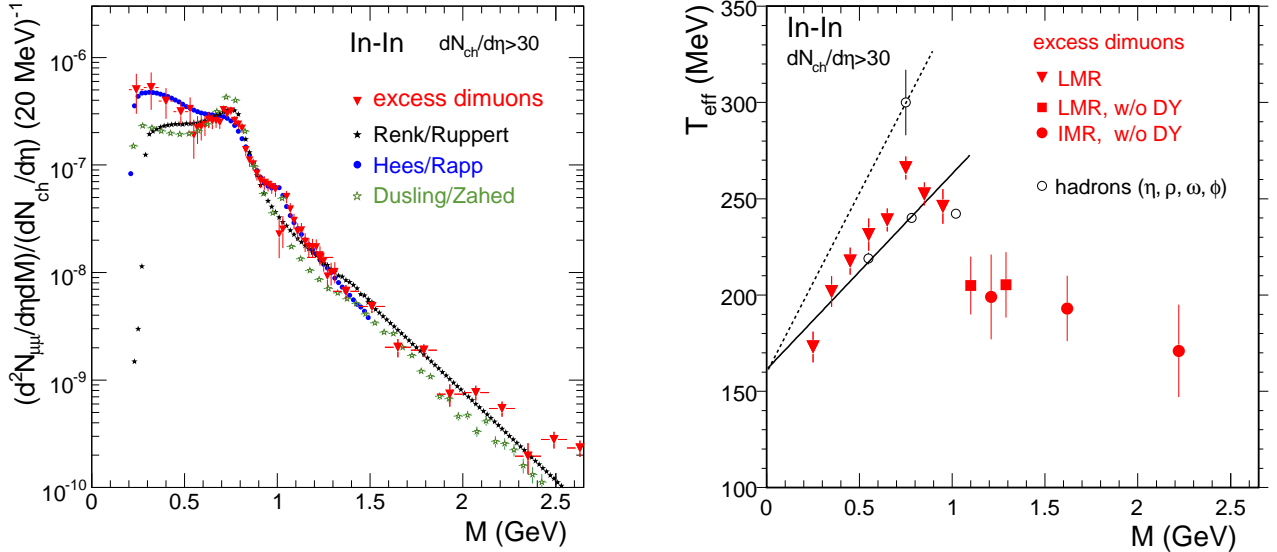


Figure 5: Left: Acceptance-corrected mass spectra of the excess dimuons for the combined LMR/IMR regions. The theoretical scenarios are labeled according to the authors RR [19], HR [20], and DZ [21]. In case of [20], the EoS-B⁺ option is used. Right: Inverse slope parameter T_{eff} vs. dimuon mass for the combined LMR/IMR regions of the excess in comparison to hadrons [13]. Open charm is subtracted in both parts of the figure.

moment of decoupling, dileptons are continuously emitted during the evolution, sensing the space-time development of temperature and flow. This makes the dilepton p_T spectra sensitive to the emission region, providing a powerful diagnostic tool [5, 19]. Fig. 4 (left) displays the centrality-integrated m_T spectra, where $m_T = (p_T^2 + M^2)^{1/2}$, for four mass windows; the ϕ is included for comparison. The ordinate is normalized to $dN_{ch}/d\eta$ in absolute terms [14, 15]. Apart from a peculiar rise at low m_T (<0.2 GeV) for the excess spectra (not the ϕ) which only disappears for very peripheral collisions [10, 13], all spectra are pure exponentials, but with a mass-dependent slope. Fig. 4 (right) shows a more detailed view into the ρ -like mass window, using the same side-window method as described in connection with Fig. 2 to determine the p_T spectra separately for the ρ peak and the underlying continuum. All spectra are purely exponential up to the cut-off at $p_T=3$ GeV, without any signs of an upward bend characteristic for the onset of hard processes. Their slopes are, however, quite different (see below).

The inverse slope parameters T_{eff} extracted from exponential fits to the m_T spectra (with a finer binning than in Fig. 4) are plotted in Fig. 5 (right) vs. dimuon mass, unifying the data from the LMR and IMR regions. The hadron data for η , ω and ϕ obtained as a by-product of the cocktail subtraction are also included, as is the single value for the ρ -peak from Fig. 4 (right). Interpreting the latter as the freeze-out ρ without in-medium effects, all four hadron values together with preliminary π^- data from NA60 can be subjected to a simple blast-wave analysis [14]. This results in a reasonable set of freeze-out parameters of the fireball evolution and suggests the following consistent interpretation of the hadron and dimuon data together. Maximal flow is reached by the ρ , due to its maximal coupling to pions, while all other hadrons freeze out earlier. The T_{eff} values of the dilepton excess rise nearly linearly with mass up to the ρ -pole position, but stay always well below the ρ line, exactly what would be expected for *radial flow* of an *in-medium hadron-like* source (here $\pi^+\pi^-\rightarrow\rho$) decaying continuously into dileptons.

Beyond the pole region of the ρ , however, the T_{eff} values of the excess show a sudden decline by about 50 MeV. Extrapolating the lower-mass trend to beyond the ρ , such a fast transition to a seeming low-

flow situation is extremely hard to reconcile with emission sources which continue to be of dominantly hadronic origin in this region. A more natural explanation would then be a transition to a dominantly early *partonic* source with processes like $q\bar{q} \rightarrow \mu^+\mu^-$ for which flow has not yet built up [19]. While still controversial [20], this may well represent the first direct evidence for thermal radiation of partonic origin, overcoming parton-hadron duality for the *yield* description in the mass domain.

The acceptance- and efficiency-corrected data can also be projected on the mass axis. The p_T -differential results are discussed in [14, 15]. Fig. 5 (left) shows p_T -integrated data for $p_T > 0.2$ GeV (the lowest p_T bin has been excluded to avoid the very large errors in the low-acceptance region [14, 15]). The LMR and IMR regions are again unified, using an independently assessed absolute normalization [22]. Recent theoretical results from the three major groups working in the field are included for comparison [19, 20, 21]. A strong rise towards low masses is seen in the data, reflecting the Boltzmann factor, i.e. the Planck-like radiation associated with a very broad, nearly flat spectral function. Only the Hees/Rapp scenario [20] is able to describe this part quantitatively, due to their particularly large contribution from baryonic interactions to the low-mass tail of the ρ spectral function. The ρ pole remains visible, due to the freeze-out part. In-medium broadening of parts of the ω and ϕ are contained in [20], but not in [19, 21], accounting for the broad bump seen in the region of the ϕ . Caution should, however, be taken as to the nearly quantitative agreement with the data, since some details of the resolution function of the NA60 apparatus are still under investigation.

Real photons and low-mass dileptons

Processes contributing to dilepton production at very low masses include $\pi\pi$ annihilation (extending to below $2M_\pi$ because of the softening of the pion dispersion relation), π -baryon processes, the a_1 -Dalitz decay, parton annihilation, internal conversion of photons from processes creating also real photons (e.g. Compton-like graphs or bremsstrahlung), and others [19, 20, 21], and the superposition of all

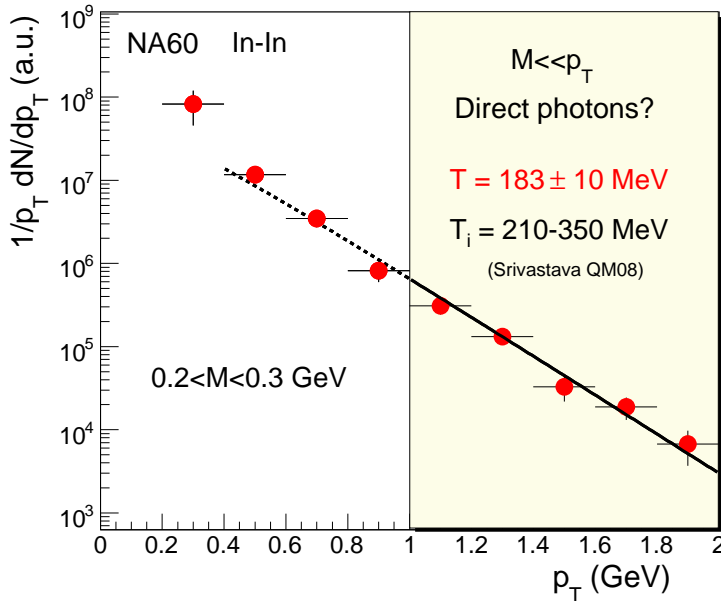


Figure 6: Acceptance-corrected p_T spectrum of the excess for the lowest mass bin $0.2 < M < 0.3$ GeV. The solid line corresponds to an exponential fit (as in Fig. 4) for $p_T > 1$ GeV, while the dashed line is just an extrapolation down to $p_T < 1$ GeV.

these sources accounts for the total measured yield as shown in Figs. 1 and 5. PHENIX at RHIC has recently [23] analysed dielectron data in the mass window $0.2 < M < 0.3$ GeV for $p_T > 1$ GeV under the extreme assumption, that the total yield for that selection would solely be due to internal conversion of real photons; the transformation back to real photons was done with the prescription in [24]. The analogous situation for NA60 is illustrated in Fig. 6, but with the complete p_T -spectrum; it corresponds to the lowest point in Fig. 5 (right). The fit value for the cut $p_T > 1$ GeV is $T = 183 \pm 10$ MeV. However, this value of T corresponds to the effective temperature T_{eff} as used in Fig. 5, affected by radial flow

(ignored by PHENIX). If corrected for that, using the intercept of the linear rise with the ordinate, it is reduced to about 150 MeV. Such a low value hardly makes sense in the light of initial temperatures of 210-350 MeV expected for real photons [25], but is more indicative for the average temperature of the hadronic phase alone. In Fig. 5, the lowest point does not look exceptional at all, but just appears as part of the general systematic rise of T_{eff} vs. mass. The lack of any convincing tag on internal conversion and the embeddment of the lowest mass bin in the general systematics rule out the real photon hypothesis for this bin, and this will hardly change at higher masses.

Conclusions

Excess dileptons have been observed over the complete mass region $0.2 < M < 2.6$ GeV. Their p_T spectra offer a clear view of the origin of the different sources. All observations, including the finding of zero polarization, are consistent with a global interpretation of the excess as thermal radiation. There is no way to unambiguously isolate real photons via internal conversion of low-mass dileptons.

References

- [1] R. D. Pisarski, *Phys. Lett. B* 110B (1982) 155
- [2] R. Rapp and J. Wambach, *Adv. Nucl. Phys.* 25 (2000) 1
- [3] G. E. Brown and M. Rho, M. M. Nagels, *Phys. Rep.* 363 (2002) 85
- [4] L. D. McLerran and T. Toimela, *Phys. Rev. D* 31 (1985) 545
- [5] K. Kajantie, M. Kataja, L. D. McLerran and P. V. Ruuskanen, *Phys. Rev. D* 34 (1986) 811
- [6] G. Agakichiev *et al.* (CERES Collaboration), *Nucl. Phys. A* 698 (2002) 539 , and earlier ref.
- [7] D. Adamova *et al.* (CERES Collaboration), *Phys. Lett. B* 666 (2008) 425
- [8] M. C. Abreu *et al.* (NA38/NA50 Collaboration), *Eur. Phys. J. C* 41 (2005) 475 , and earlier ref.
- [9] A. L. S. Angelis *et al.* (HELIOS-3 Collaboration), *Eur. Phys. J. C* 13 (2000) 433 , and earlier ref.
- [10] H. J. Specht, *Nucl. Phys. A* 805 (1985) 338 , preprint arXiv:0710.5433
- [11] R. Arnaldi *et al.* (NA60 Collaboration), *Eur. Phys. J. C* (2009) in press , preprint arXiv:0810.3204
- [12] R. Arnaldi *et al.* (NA60 Collaboration), *Phys. Rev. Lett.* 96 (2006) 162302
- [13] R. Arnaldi *et al.* (NA60 Collaboration), *Phys. Rev. Lett.* 100 (2008) 022302
- [14] S. Damjanovic *et al.* (NA60 Collaboration), *J. Phys. G* 35 (2008) 104036 , preprint arXiv:0805.4153
- [15] R. Arnaldi *et al.* (NA60 Collaboration), *Eur. Phys. J. C* (2009) in press , preprint arXiv:0812.3053
- [16] S. Damjanovic *et al.* (NA60 Collaboration), *Eur. Phys. J. C* 49 (2007) 235
- [17] R. Rapp, 2003, private communication and R. Rapp, nucl-th/0204003
- [18] S. Damjanovic *et al.* (NA60 Collaboration), *Nucl. Phys. A* 783 (2007) 327
- [19] J. Ruppert, C. Gale, T. Renk, P. Lichard and J. I. Kapusta, *Phys. Rev. Lett.* 100 (2008) 162301 ; T. Renk and J. Ruppert, *Phys. Rev. C* 77 (2008) 024907
- [20] H. van Hees and R. Rapp, *Phys. Rev. Lett.* 97 (2006) 102301 ; H. van Hees and R. Rapp, *Nucl. Phys. A* 806 (2008) 339 and earlier ref.; H. van Hees *J. Phys. G* 35 (2008) 104034
- [21] K. Dusling, D. Teaney and I. Zahed, *Phys. Rev. C* 75 (2007) 024908 ; K. Dusling and I. Zahed, preprint hep-ph/0701253
- [22] R. Shahoyan *et al.* (NA60 Collaboration), Proceedings of the PANIC 2008 Conference
- [23] A. Adare *et al.* (PHENIX Collaboration), preprint arXiv:0804.4168 [nucl-ex]
- [24] N. M. Kroll and W. Wada, *Phys. Rev.* 98 (1955) 1355
- [25] D. K. Srivastava, *J. Phys. G* 35 (2008) 104026